PAPER • OPEN ACCESS

Shape Memory Alloys: identification of the parameters necessary for constitutive models

To cite this article: A K Elwaleed 2018 *IOP Conf. Ser.: Mater. Sci. Eng.* **453** 012027

View the article online for updates and enhancements.

Shape Memory Alloys: identification of the parameters necessary for constitutive models

A K Elwaleed[1]

Mechanical Engineering Department, Jubail University College P. O. Box 10074, Jubail Industrial City 31961, Kingdom of Saudi Arabia

E-mail: khidire@ucj.edu.sa

Abstract. The purpose of this research is to identify the Shape Memory Alloy (SMA) parameters necessary for SMA actuators analysis using SMA constitutive models. The behavior of a material is primarily a function of three variables: stress, strain and temperature, and their associated rates. These variables are interdependent, and the material behavior is a non-linear function of these variables. A number of constitutive models for shape memory alloys have been proposed and found to be relatively convenient to use in predicting and describing shape memory alloys' behaviors quantitatively. However, the application of these models in designing and analyzing an actuator requires the determination of the thermomechanical properties of these materials such as transformation temperatures, thermoelastic tensor, Young's modulus, Transformation tensor) and recovery strain. This research has been conducted to identify the thermomechanical properties of a commercial NiTi SMA wire. The paper shows in details how these parameters can be identified.

1. Introduction

There are many types of smart materials, such as shape memory alloys, piezoceramics, electrostrictive and electroactive polymers, mechano-chemical polymer/gels, etc. However, SMA actuators can attain a high strength to weight ratio, which makes them ideal for miniature application [1]. From a mass and volume saving point of view, Hirose et al. [2] have compared the power/weight ratio vs. weight of a particular form of SMA actuator with many other conventional motors. It suggested that SMA actuators have the potential capability to achieve a better output/weight ratio compared with traditional actuators.

Shape memory effect refers to the ability of certain materials to recover a predetermined shape when heated. When a SMA is in the martensite phase at low temperature, it has a very low yield strength and can be deformed quite easily into a new shape, which it retains. However, when the material is heated so that it is in the austenitic phase at high temperature, the SMA undergoes a change in crystal structure, which causes it to return back to its original shape. Some examples of these alloys are Ag-Cd, Au-Cd, Cu-Al-Ni, Cu-Zn, Ni-Al, Ni-Ti, Fc-Pt and Mn-Cu, [3]. SMAs considered attractive candidate materials for applications in actuators because of their dual functionality of sensing and actuating in a single body [4]. The simplicity of their actuation principle and their compatibility with micro system technologies make them very attractive for highly miniaturized and micro-electromechanical systems. Consequently many SMA micro-actuator applications have been tested to build innovative biomedical instruments like endoscopes, steerable catheters, forceps, grippers, prosthetic devices, orbit floor implant [5, 6].

Large forces can be generated with these actuators, as the stress limit is more than 250 MPa for working conditions [7]. Several researchers have implemented shape memory alloy technology for use in articulated hands and fingers [8-12].

Although shape memory alloys have very large force generation and light weight compared with the conventional actuators but they suffer from hysteresis that makes the actuators difficult to model and control and they are also known for their limited strain. They can deform up to 5% workable strain. To obtain a higher strain this needs a mechanical amplification. The amplifications can be obtained normally by using long SMA wires or SMA coils. The long wires occupy long space which is not suitable for miniature applications. Coils suffer from debilitating drawback of requiring a larger diameter than necessary [13].

Many experimental and innovative uses of SMA actuators have been proposed but there is still a need for a design-oriented thermomechanical model of SMA actuators for the mechanical optimization as well as for simulation of micro/miniaturized structures. Among all the design principles based on SMA-actuation, the use of wires offers several possibilities of actuator structures and makes them of particular interest. NiTi alloy show the best mechanical characteristics among the number of alloys and polymers, which exhibit a shape memory effect.

2. Shape Memory Alloy Transformation and Constitutive Response

Shape Memory Alloys (SMAs) transform due to mechanical or thermal loading. The martensite to austenite transformation is known as the reverse transformation. The austenite to martensite transformation is known as the martensitic transformation. Martensite transformations are of first order, meaning that heat is liberated when martensite is formed [14]. There is a hysteresis associated with the transformation and there is temperatures range over which both coexist. Crystallographically, the transformation from austenite to martensitic transformation occurs by two processes: Bain strain and lattice-invariant shear (Figure 1). The behavior of a material is primarily a function of three variables: stress, strain and temperature, and their associated rates. These variables are interdependent, and the material behavior is a non-linear function of these variables [15, 16]. Out of all shape memory alloys so far, NiTi has proven to be the most flexible and beneficial in engineering applications [17]..
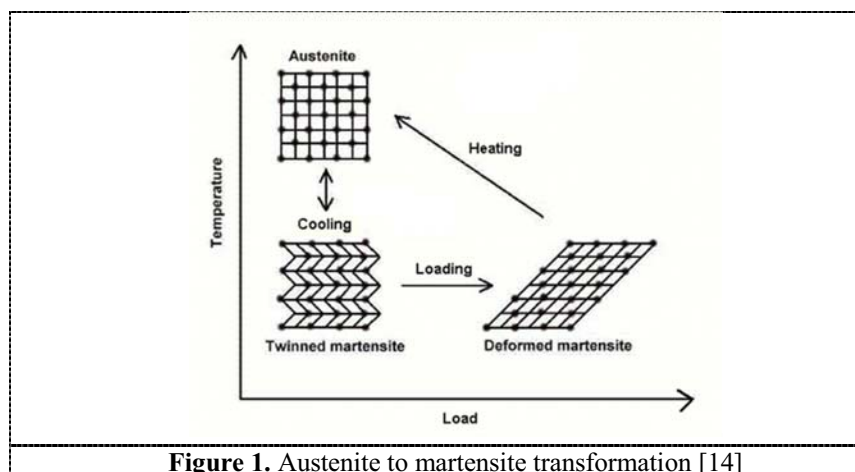

Figure 1. Austenite to martensite transformation [14]

3. Constitutive Models

The modeling of the thermomechanical behaviors of SMA has been an active area of research over the past decades. Prediction of SMA behaviour involves formulating a model that describes the state of the material in terms of its three primarily variables – stress, strain and temperature [18]. There are two approaches to establish a constitutive relation for any material. One is the macroscopic phenomenological method that requires a significant amount of experimental work; the other is the microscopic physical method that derives the constitutive relation from physical concepts. The phenomenological approach is often used in engineering practice; however, it can rarely explain the physics behind the material's behavior or character. The microscopic physical method can successfully provide the fundamental explanation to different experimental phenomena; however, its numerical predictions and simulations are often complex and distant from phenomenological observations.

A number of constitutive models for shape memory alloys have been proposed. Tanaka, Liang and Rogers, and Brinson models are found to be relatively convenient to use in predicting and describing shape memory alloys' behaviours quantitatively [18-21]. The three models use an internal variable, ξ, to represent the extent of a martensitic transformation. Among the three models, Brinson model has the advantage of being capable of capturing the unique thermomechanical behavior of SMAs at all temperatures [22].

3.1. Tanaka Model [19]

Tanaka developed a model in 1982, which is basically governed by the minimization of the free energy. This model has been used to study superelasticity [23], pseudoelasticity, and SMA materials (Tanaka [20], qualitatively. This model describes the state variables – stress (σ) strain (ε) and temperature (T) in terms of a martensitic volume fraction (ξ). The constitutive equation is:

$$\sigma - \sigma_o = D(\xi)(\varepsilon - \varepsilon_o) + \Theta(T - T_o) + \Omega(\xi)(\xi - \xi_o) \tag{1}$$

where the subscript 'o' refers to the initial state of the material, D refers to the modulus of elasticity, and Ω is a constant called the phase transformation coefficient. The modulus E is assumed to be a linear function of the martensite volume fraction,

$$D(\xi) = D_A + \xi (D_M - D_A) \qquad \text{and} \qquad \Omega(\xi) = -\varepsilon_L D(\xi) \tag{2}$$

where ε_L is the maximum recoverable strain. Tanaka's model assume an exponential function for the martensite volume fraction:

During the M $\leftarrow$ A transformation, the martensite volume fraction is modeled as:

$$\xi = 1 - \exp\{(a_M (M_A - T) + b_M \sigma\} \tag{3}$$

and during the M $\rightarrow$ A transformation,

$$\xi = \exp\{(a_A (A_S - T) + b_A \sigma\} \tag{4}$$

The empirical constants used to describe the particular material are:

$$a_A = \frac{\ln(0.01)}{(A_S - A_f)}, \qquad b_A = \frac{a_A}{C_A}, \qquad a_M = \frac{\ln(0.01)}{(M_S - M_f)} \quad \text{and} \quad b_M = \frac{a_M}{C_M}$$

The stress-influence coefficients, C_A and C_M are the slope of the critical stress-temperature plot, which shows the variation of the transformation temperatures with stress, as illustrated in Figure 2.
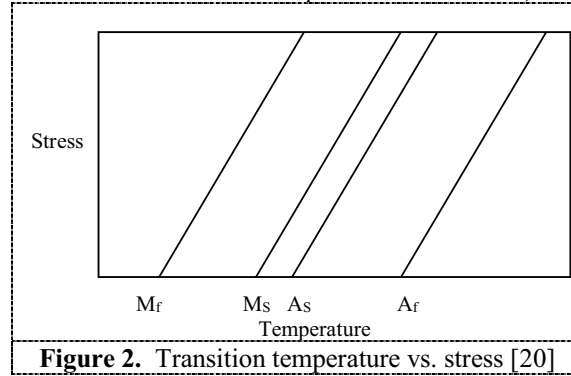

Figure 2. Transition temperature vs. stress [20]

3.2. Liang and Rogers Model [18]

This model has the same form of constitutive equation as the Tanaka model, except that a cosine function is used to model the martensite volume fraction. Some of the constants are also defined differently. For the M $\leftarrow$ A transformation, the martensite fraction is:

$$\xi = \frac{(1 - \xi_A)}{2} \cos\{a_M (T - M_f) + b_M \sigma\} + \frac{(1 + \xi_A)}{2} \tag{5}$$

and for the M $\rightarrow$ A transformation, it is defined as

$$\xi = \frac{(\xi_M)}{2} \{\cos[a_A (T - A_S) + b_A \sigma] + 1\}$$

where

$$a_A = \frac{\pi}{(A_S - A_f)}, b_A = \frac{a_A}{C_A} \qquad a_M = \frac{\pi}{(M_S - M_f)}, b = \frac{a_M}{C_M}$$

ξ_A and ξ_M are the initial volume fraction for the M←A and M→A transformations respectively, usually obtained by assuming an initial starting phase. Other symbols represent the same as in Tanaka's model.

3.3. Brinson's Model [21]
Brinson proposed a separation of the internal variable ξ into two parts as

$$\xi = \xi_{Ss} + \xi_T \tag{6}$$

where ξ_T represents the fraction of the material that is purely temperature-induced martensite, and ξ_S the fraction of the material that has been transformed by stress into detwinned martensite, or stress-induced martensite. The stress-induced martensite contributes to the global strain of the material, while the purely temperature-induced martensite does not. With this proposition and based on Liang and Roger model, the constitutive relation of SMAs with constant material function is

$$\sigma - \sigma_0 = D(\varepsilon - \varepsilon_0) + \Omega (\xi_S - \xi_{S0}) + \Theta(T - T_0) \tag{7}$$

D, Ω and recoverable strain limit ε_L are related by:

$$\Omega = -\varepsilon_L D \tag{8}$$

σ_s^{cr} and σ_f^{cr} are the critical stresses at the start and finish of the conversion of the martensite variants at the temperature below M_s. Constants a_M and a_A are defined by

$$a_A = \pi / (A_f - A_s) \qquad\qquad a_M = \pi / (M_s - M_f)$$

4. Parameters Identification Of Shape Memory Alloy
It is necessary to understand the thermomechanical properties of these materials, to design an actuator using shape memory alloys (SMA). The quasistatic behavior of an SMA is a function of three primary variables – stress, strain and temperature.

Transformation temperatures, M_f (martensite finish) M_s (martensite start), A_s (austenite start) and A_f (austenite finish), are measured using Differential Scanning Calorimeter (DSC). Except for the thermoelastic tensor (Θ), which needs to be measured from a constraint recovery, all the other material constants D (Young's modulus), Ω (Transformation tensor) and ε_L (recovery strain) were determined from isothermal tensile testing at various temperatures [24]. The details on the determination of these material constants are described by Liang & Rogers [18].

4.1. Transformation Temperatures
The experiments were performed on a commercial NiTi (55.2 wt.% Ni, 44.7 wt.% Ti and less than 0.1% other elements) wire of 0.7 mm diameter. Heat treatment was done for four samples of NiTi shape memory alloy wire. The samples were annealed at 500°C, 600°C, 700°C and 800°C for 30 minutes and then quenched in water at the room temperature (28.5°C).

The DSC result for the wires treated at 800°C is shown in Figures 3. It was observed that the wires treated at 800°C, 700°C and 600°C have four transformation temperatures for the wire to transform from martensite phase to austenite phase or vise versa (M_s, M_f, A_s and A_f). However, the wire treated at 500°C had one trough and two peaks in which a third phase called "rhombohedral phase" existed between the martensite and the austenite phases and it has two transformation temperatures (R_s and R_f). Table 1 shows the transformation temperatures for the four wires. The rhombohedral phase transformation can give rise to a second shape memory mechanism [25]. Although the R-phase transition has an advantage of having small hysteresis of around 1.5°C, compared with the martensite temperature hysteresis which can reach up to 10°C, but it suffers of giving more than 0.5% recoverable strain.

This study shows that as annealing temperature increases austenite start, austenite finish, martensite start and austenite finish increase. From the heat treatment and DSC tests for the wire, it can be concluded that the most suitable heat treatment temperature is above 700 °C in which the rhombohedral phase is eliminated and the martensite phase temperatures are within the room temperature ranges.
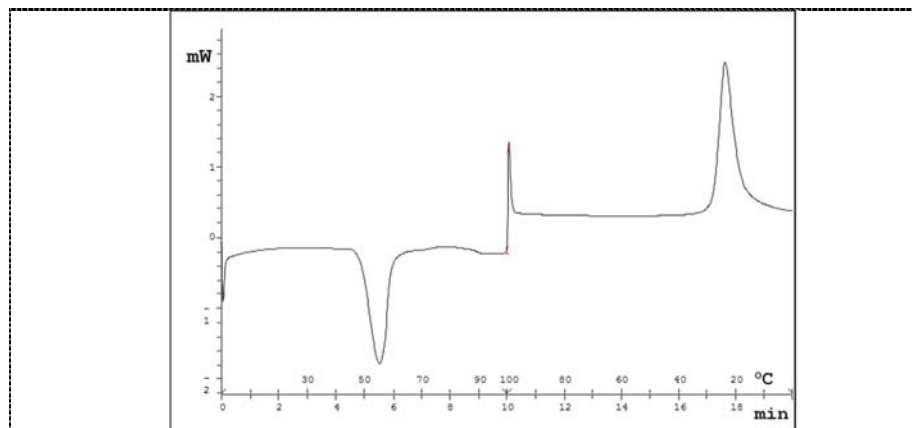
Figure 3 DSC for the SMA wire heat treated at 800°C for 30 minutes and quenched in water at room temperature 28.5°C

Table 1. Transformation temperatures for NiTi SMA wire heat treated at different temperatures for 30 minutes

Heat Treatment Temperature (°C)	Transformation Temperatures (°C)					
	M_f	M_s	R_f	R_s	A_s	A_f
800	16	27.2	-	-	49.2	60
700	15.2	24.6	-	-	48.3	58.8
600	13.2	20	-	-	46.3	55.3
500	-15.6	-8.4	21.4	26.1	26.3	31

4.2. SMA Wire Training

To predict the thermo-mechanical properties of the SMA, it was necessary to carry out careful testing of the SMA wire to determine coefficients for the constitutive models. Systematic specimen testing is essential since there is no reliable database available for the properties of SMA materials and also the thermo-mechanical properties of the shape memory alloys depend on many variables such as wire manufacturing, wire diameter, pre-strain, stress level, temperature, and wire training.

In this research the specimens were trained prior to testing to stabilize the shape memory effect for each specimen and to ensure repeatable characteristics and uniformity. Cycling the wire involved clamping the wire at both ends using the Testometric tensile machine. The training procedure consisted of extending the wire to a strain of about 5% at an elongation speed of 0.5 mm/sec, and then releasing the wire to zero stress. The wire was strained at low temperature while it was in the martensite phase. This is followed by heating the wire to a temperature above the austenite finish temperature (A_f), to recover the deformation, and then cooled down to below martensite finish temperature (M_f). Deforming the wire and recovery of the deformation comprise one cycle. Each wire sample was typically trained 40 times. Figure 4 shows the results of training a shape memory alloy wire sample. From the figure it can be observed that the residual strain is fluctuating and unstable up to 30 number of cycles. However, after about 30 cycles no significant deviation in the characteristics of the SMA wire were observed.

4.3. Young's Moduli

The Young's moduli of the austenite phase (D_A) and the martensite phase (D_M) were determined from the stress strain curves (Figure 5). The tests were carried out using the tensile tester equipped with a controlled temperature chamber. D_A was obtained at a constant temperature of 85°C while D_M was obtained at the constant temperature of 30°C. The moduli, measured from the slope of elasticity at temperatures where the specimen is in proper phase, are: $D_A = 34$ GPa   and $D_M = 12$ GPa.
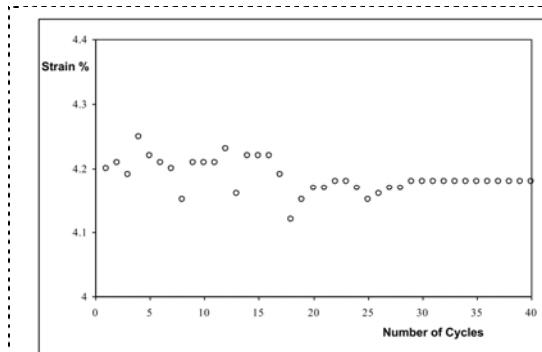
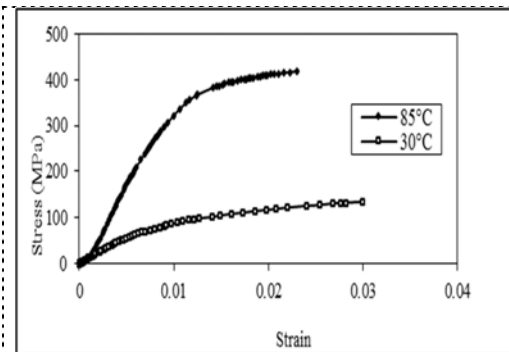| **Figure 4.** Training results of SMA wire residual strain versus number cycles	**Figure 5.** Stress-strain relationship when loading the SMA wire at 30°C and 85°C

4.4. Recovery Strain

The maximum recoverable strain ε_L, is determined from the residual strain after unloading from the end of the initial yielding plateau. The value for the recoverable strain was found to be 6.95%.

4.5. Transformation Coefficient

Knowing ε_L and D, the transformation coefficient, Ω, can be calculated using the relationship, $\Omega = -D\varepsilon_L$ [18], for the martensite, $\Omega_M = -D_M \varepsilon_L$, for the austenite, $\Omega_A = -D_A \varepsilon_L$.

4.6. Stress Influence Coefficient

A resistivity test fixture is needed to set up to allow the measurement of the transformation function under constant loads for the measurement of the stress influence coefficient, C. (Figure 6). From the figure the following result is obtain:

$$C_M = 7 \text{ MPa/°C} \quad \text{and} \quad C_A = 6.3 \text{ MPa/°C}$$
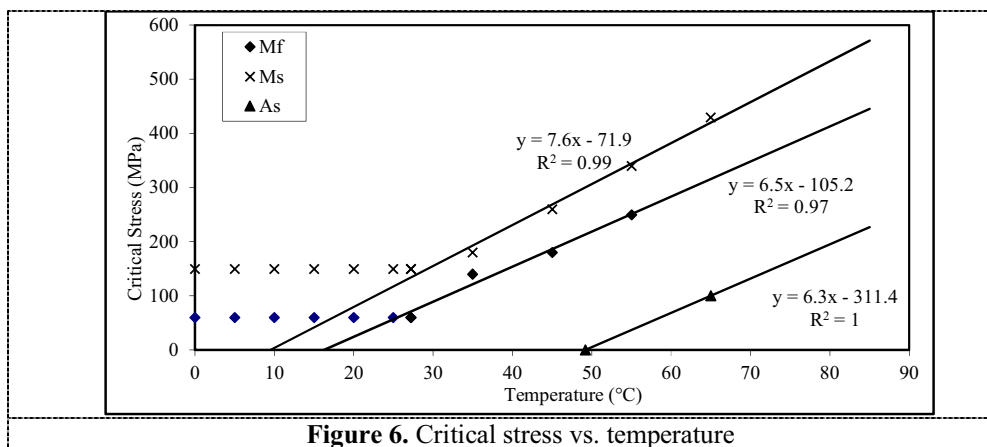

Figure 6. Critical stress vs. temperature

4.7. Stress Influence Coefficient

The recovery stress has a linear relation with temperature for temperature higher than the mechanical austenite finish temperature (A_f^m). This point is observed in the experimental results shown in Figure 8. The thermoelastic coefficient ($\varTheta$) was determined by restrained recovery test and by heating the wire above the austenite finish temperature. The coefficient is obtained from the slope of stress temperature curve above this temperature as shown in Figure 7. It was found to be equals to 2.79 MPa/°C.

4.8. Critical Stresses
Figure 8 displays a typical tensile stress-strain curve for a shape memory material. There are two "yield" plateaus associated with the constitutive behavior. The first occurs due to the onset of detwinning of the martensite variants. At the end of this plateau the martensite variants are fully detwinned and elastic deformation of the self-accommodated martensitic variant begins to occur. At the second plateau, slip and dislocation movement occur [23].

The critical stresses are usually found for a given material by uniaxial tension tests and then picking the initial knee in the stress-strain curve to be the critical start stress (σ_s^{cr}) for transformation. The second knee is the critical finish stress (σ_f^{cr}).

From figure 8, the critical stresses are as follows:

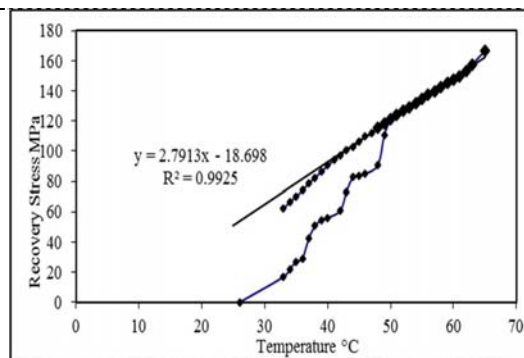$$\sigma_s^{cr} = 60 \text{ MPa} \qquad \text{and} \qquad \sigma_f^{cr} = 150 \text{ MPa}$$

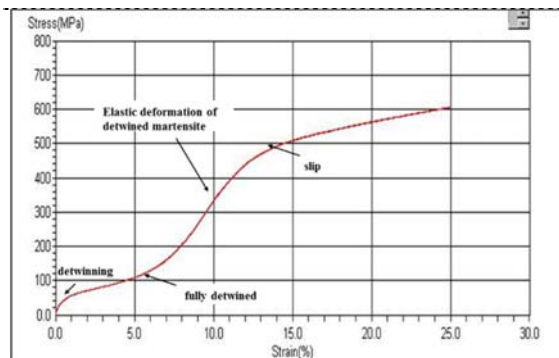**Figure 7.** Recovery stress vs. temperature

Figure 8. Typical SMA constitutive behavior

Table 2 summarizes the thermomechanical properties of the used shape memory alloy wire and other necessary parameters for designing shape memory alloy actuators.

Table 2. SMA wire parameters

Parameter	Description	Value
M_s	Martensite start temperature	16°C
M_f	Martensite finish temperature	27°C
A_s	Austenite start temperature	49°C
A_f	Austenite finish temperature	60°C
D_M	Martensite Young modulus	12 MPa
D_A	Austenite Young modulus	34 MPa
C_M	Martensite stress influence coefficient	7 MPa/°C
C_A	Austenite stress influence coefficient	6.3 MPa/°C
ε_L	Recoverable strain	6.95%
Ω_M	Martensite transformation coefficient	0.834 MPa
Ω_A	Austenite transformation coefficient	2.363 MPa
Θ	Thermoelastic tensor	2.79 MPa/°C
σ_s^{cr}	Critical start stress	60 MPa
σ_f^{cr}	Critical finish stress	150 MPa

5. Conclusions
This paper shows in details how the thermomechanical parameters necessary for SMA actuators can be identified. The parameters are transformation temperatures, thermoelastic tensor, Young's modulus, Transformation tensor) and recovery strain. This research has been conducted to identify the

thermomechanical properties of a commercial NiTi SMA wire. The parameters are very important in designing and analysing SMA actuators.

References
[1]   Ikuta K 1990 *In IEEE Robotics and Automation Society*, Los Alamitos, California, *3* 2156.
[2]   Hirose S, Ikuta K and Umetani Y 1985 *Proc. of RoManSy, The Fifth CISM-IFToMM Symposium.* Cambridge, MA: The MIT Press, pp. 339-349.
[3]   Mosley M, Mavroidis C and Pfeifer C 1999 *Proc. of the ANS, 8th Tropical Meeting on Robotics and Remote Systems*, Pittsburgh, PA.
[4]   Nam T, Yu C, Lee Y J and Liu Y 2006 *International Journal of Applied Electromagnetics and Mechanics* **23** 9.
[5]   Loh C S, Yokoi H and Arai T 2005 *Proc. of the 2005 IEEE Engineering in Medicine and Biology 27th Annual Conference,* Shanghai, China, pp. 6900-6903.
[6]   Grunert   R,   Lichtenstein   J,   Preßler   N,   Geßner   M,   Rotsch   C, Wagner M, Posern S, Pabst F, Drossel W 2016 *Procedia CIRP* **49** 143.
[7]   Grant D and Hayward V 1995 *Proc. of IEEE International Conference on Robotics and Automation* **3** 2305.
[8]   Dario P Bergamasco, M Bernardi L and Bicchi A 1987 *In IEEE Micro Robots and Teleoper-actuation Workshop.* Hyannis, MA, IEEE Robotics and Automation Council.
[9]   Gharaybeh, M A and Burdea G C 1995 *Advanced Robotics* **9** 317.
[10]   Hashimoto M, Takeda M, Sagawa H, Chiba I and Sato K 1985 *Journal of Robotic Systems* **2** 3.
[11]   Chaudhuri P and Fredericksen D H 1985 *IBM Technical Disclosure Bulletin* **28** 302.
[12]   Nakano Y, Fujie M and Hosada Y 1984 *Robotics Age* **6** 18.
[13]   Grant D. and Hayward V 2000 *Proc.of the 2000 IEEE International Conference on Robotics and Automation*, San Francisco, CA pp. 1314.
[14]   Duerig T W, Melton K N, Stockel D and Wayman C M 1990 *Engineering Aspects of Shape Memory Alloys* (London, Butterworth-Heinemann).
[15]   Sun Q P and Hwang K C 1993 *Journal of the Mechanics and Physics of Solids* **41** 1.
[16]   Hebda D A and White S R 1994 *ASME Winter Annual Meeting, Symposium on Adaptive Structures and Materials,* Chicago II, pp. 6-11.
[17]   Waram T 1993 *Actuator Design Using Shape Memory Alloys.* 2nd Edition. Ontario, Canada, TC.
[18]   Liang C and Rogers C A 1990 *Journal of Intelligent Material Systems and Structures* **1** 207.
[19]   Tanaka K and Nagaki S 1982 *Ingenieur-Archiv* **51** 299.
[20]   Tanaka K 1986 *Research Mechanica* **18** 263.
[21]   Brinson L C 1992 *Proc. Conf. on Recent Advances in Adaptive Sensory Materials and their Applications* (Blacksburg, VA, 1992). New York: Technomie.
[22]   Ford D S, Hebta D A and White S R 1995 *In Proceedings of SPIE 31st Ann. Tech. Meeting Soc. Eng. Sci. Active Materials and Smart Structures* **2724** 218.
[23]   Tanaka K and Iwasaki R 1985 *Engineering Fracture Mechanics* **21** 709.
[24]   Lei C Y and Wu M H 1991 *Smart Structure and Materials ASME* **123** 73.
[25]   Miyazaki S and Wayman C M 1988 *Acta Metallurgica* **36** 181.